

## Supporting Information

### Ferromagnetic coupling between 4f- and delocalized $\pi$ -radical spins in mixed (phthalocyaninato)(porphyrinato) rare earth double-decker SMMs

Liguo Yang, Xin Wang, Mengliang Zhu, Tongtong Xiao, Zhongwen Ouyang,  
Yongzhong Bian, Zhenxing Wang and Jianzhuang Jiang

#### Content

1. Chemicals and instruments.
2. NMR spectra of Y<sup>III</sup>(Pc)(TNP) (**3**) in CDCl<sub>3</sub>, Figure S1.
3. Electronic absorption spectra and data of M<sup>III</sup>(Pc)(TNP) (M = Tb (**1**), Dy (**2**), Y(**3**)) in CHCl<sub>3</sub>, Figure S2 and Table S1.
4. IR spectra of **1–3**, Figure S3.
5. Crystallographic and structural data for **1**·C<sub>60</sub>, Tables S2 and S3.
6. Molecular packing in single crystals of **1**·C<sub>60</sub>, Figure S4.
7. Temperature (*T*) dependence of  $\chi_M T$  for **1** and **2** at 1000 Oe, Figure S5.

8. Plots for temperature dependence of the in-phase ( $\chi'$ ) and out-of-phase ( $\chi''$ ) ac susceptibility of **1** and **2** under a zero applied dc magnetic field, Figure S6.
9. Plots for temperature dependence of the in-phase ( $\chi'$ ) and out-of-phase ( $\chi''$ ) ac susceptibility of **1** under 2000 Oe applied dc magnetic field, Figure S7.
10. The plot of  $\ln(\tau)$  vs.  $1/T$  for **2** under 2000 Oe applied dc field, Figure S8.
11. References.

### *Chemicals and instruments*

Column chromatography was carried out on silica gel (300-400 mesh, Qingdao Ocean Chemicals) and biobeads (BIORAD S-X1 200-400 mesh) with the indicated eluents. TCB and dichloromethane were freshly distilled from CaH<sub>2</sub> under nitrogen. All other reagents and solvents were used as received. H<sub>2</sub>TNP, <sup>1</sup>Li<sub>2</sub>Pc<sup>2</sup> and M(acac)<sub>3</sub>·nH<sub>2</sub>O (M=Y, Tb, Dy)<sup>3</sup> were prepared according to the published procedure.

MALDI-TOF mass spectra were taken on a Bruker Microflex<sup>TM</sup> LRF spectrometer with dithranol as the matrix. Elemental analyses were performed on an Elementar Vario MICROCUBE elemental analyzer. <sup>1</sup>H NMR spectra were recorded on a 400 MHz NMR spectrometer in CDCl<sub>3</sub> and the chemical shifts were reported relative to internal SiMe<sub>4</sub>. Electronic absorption spectra were recorded with a Hitachi U-4100 spectrophotometer. IR spectra were recorded as KBr pellets using a Bruker Tensor 37 spectrometer with 2 cm<sup>-1</sup> resolution. The magnetic measurements were performed on SQUID-VSM with polycrystalline samples.

X-ray crystallography data were collected on an Oxford Diffraction Gemini E system with a **Cu** K $\alpha$  sealed tube ( $\lambda = 1.5418 \text{ \AA}$ ) at 150 K, using a  $\omega$  scan mode with an increment of 0.3°. Preliminary unit cell parameters were obtained from 45 frames. Final unit cell parameters were derived by global refinements of reflections obtained from integration of all the frame data. The collected frames were integrated using the preliminary cell-orientation matrix. The SMART software was used for collecting

frames of data, indexing reflections, and determination of lattice constants;<sup>4</sup> SAINT-PLUS for the integration of intensity of reflections and scaling;<sup>4</sup> SADABS for absorption correction;<sup>5</sup> and SHELXL for space group and structure determination, refinements, graphics, and structure reporting.<sup>6</sup> CCDC-1917281 contain the supplementary crystallographic data for this paper. These data can be obtained free of charge from The Cambridge Crystallographic Data Centre via [www.ccdc.cam.ac.uk/data\\_request/cif](http://www.ccdc.cam.ac.uk/data_request/cif). Crystal data and details of data collection and structure refinement are given in **Table S2**.

HF-EPR measurements were performed on a locally developed spectrometer at the Wuhan National High Magnetic Field Center, China.<sup>7,8</sup> This facility is a transmission-type instrument, in which the microwaves are propagated by oversized cylindrical light pipes. The tunable microwave frequencies were provided by the combination of Gunn oscillators (Millitech) and backward wave oscillators (Institute of General Physics, Moscow, Russian Federation). The magnetic field was generated by a pulsed field magnet, and the detection was performed with an InSb hot-electron bolometer (QMC Ltd., Cardiff, U.K.). In order to minimize the field-induced torquing effect, samples were ground, mixed with KBr, and pressed into pellets.

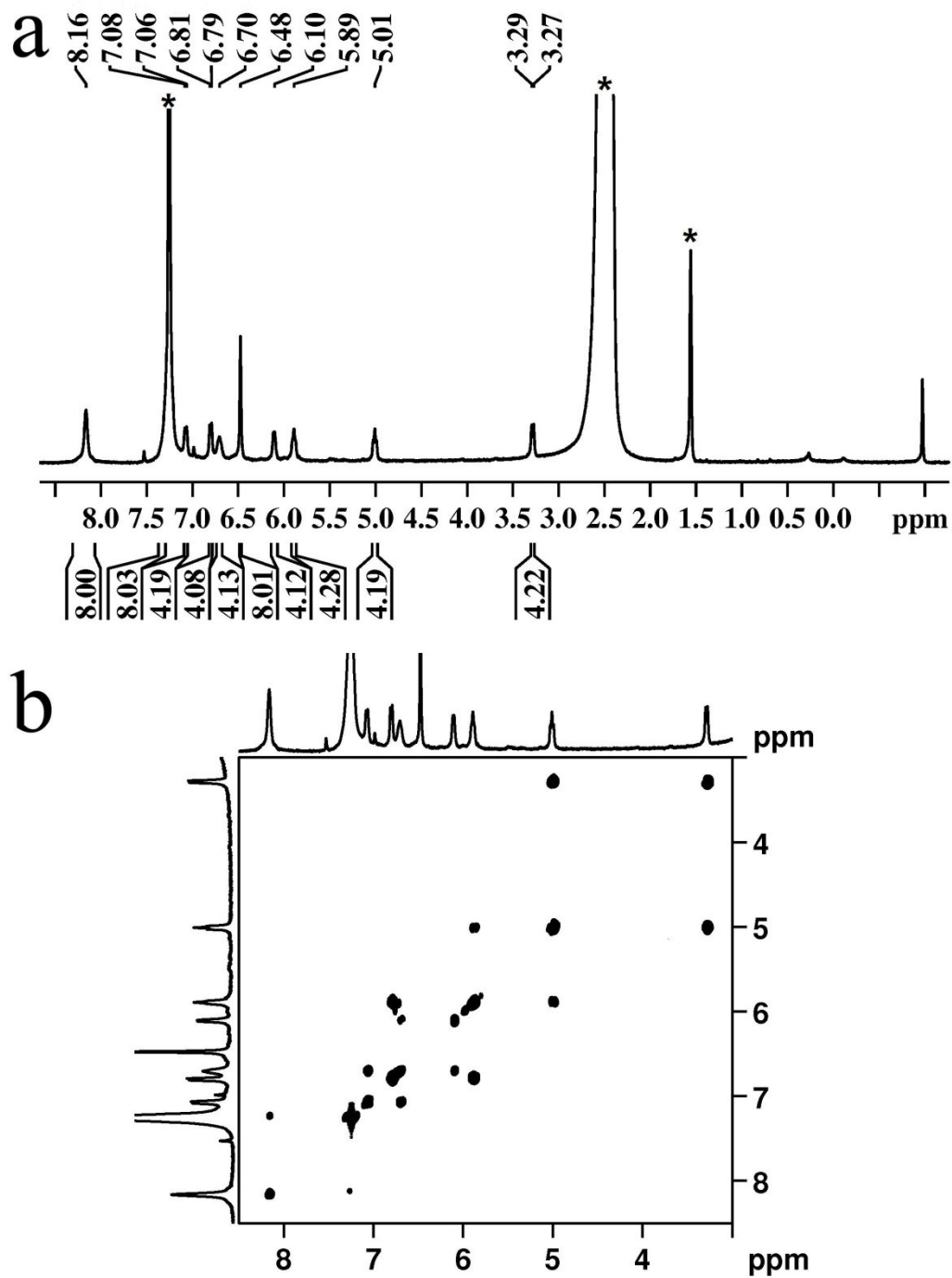


**Figure S1.** (a)  $^1\text{H}$  NMR and (b)  $^1\text{H}$ - $^1\text{H}$  COSY spectra of  $\text{Y}^{\text{III}}(\text{Pc})(\text{TNP})$  (**3**) in  $\text{CDCl}_3$  (with ca. 1% hydrazine hydrate); the asterisk (\*) indicates the signals for residual solvent.



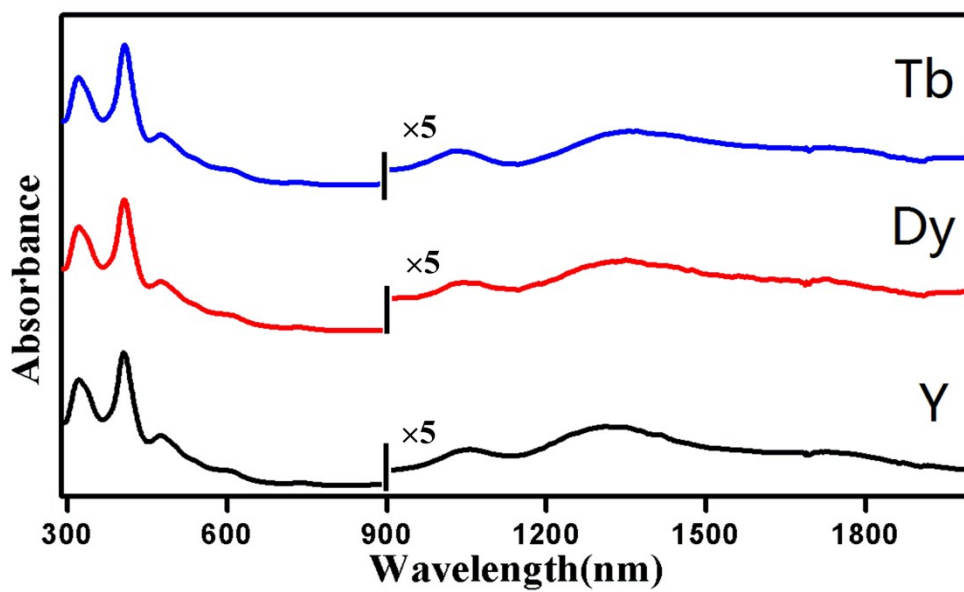


**Figure S2.** Electronic absorption spectra of  $M^{III}(\text{Pc})(\text{TNP})$  ( $M = \text{Tb}$  (1),  $\text{Dy}$  (2),  $\text{Y}$  (3)) in  $\text{CHCl}_3$ .

**Table S1.** Electronic absorption data of **1-3** in CHCl<sub>3</sub>.

compound	$\lambda_{\text{max}}/\text{nm}$ ( $\log\epsilon$ )					
Tb(Pc)(TNP) ( <b>1</b> )	320	408	464	732	1032	1363
	(4.96)	(5.07)	(4.63)	(3.61)	(3.89)	(4.21)
Dy(Pc)(TNP)	321	407	464	734	1046	1348
( <b>2</b> )	(4.95)	(5.05)	(4.81)	(3.64)	(3.91)	(4.19)
Y(Pc)(TNP) ( <b>3</b> )	322	406	464	736	1055	1323
	(4.93)	(5.01)	(4.77)	(3.69)	(3.92)	(4.23)



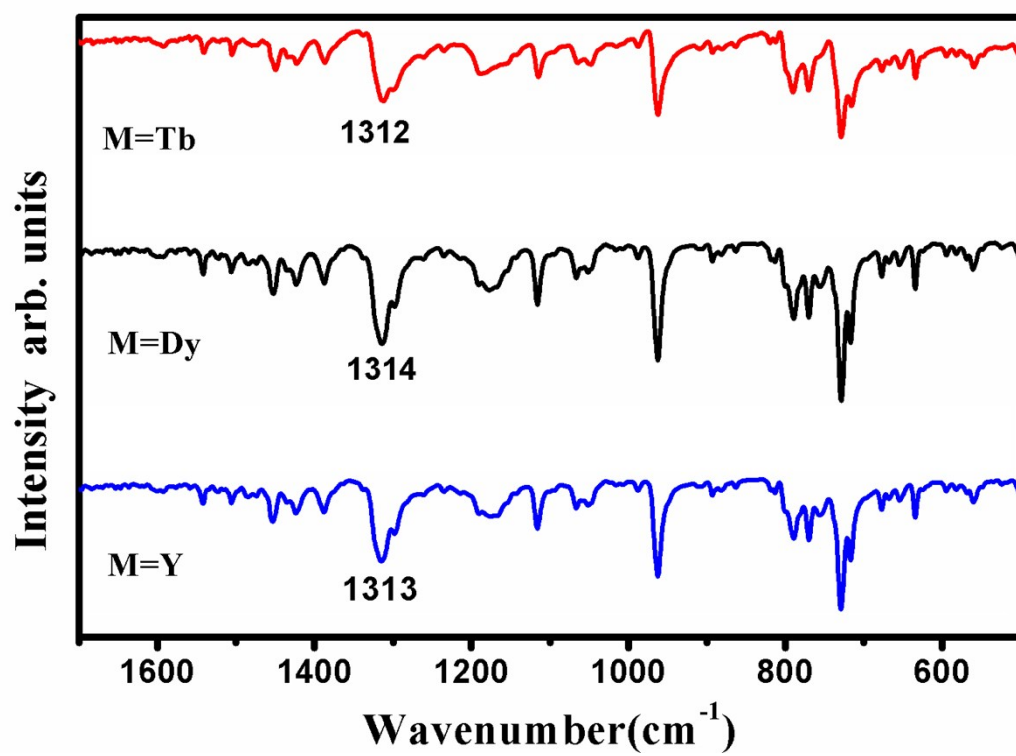


Figure S3. IR spectra of 1-3.

**Table S2.** Crystallographic data for **1·C<sub>60</sub>**.

<b>1·C<sub>60</sub></b>	
Formula	C <sub>152</sub> H <sub>52</sub> N <sub>12</sub> Tb
<i>M</i>	2204.94
Cryst syst	Trigonal
Space group	<i>R</i> -3
<i>a</i> /Å	37.4445(4)
<i>b</i> /Å	37.4445(4)
<i>c</i> /Å	42.9264(5)
<i>α</i> /deg	90
<i>β</i> /deg	90
<i>γ</i> /deg	120
<i>V</i> /Å <sup>3</sup>	52123.2(10)
<i>Z</i>	18
<i>F</i> (000)	24336
<i>D<sub>c</sub></i> /Mg m <sup>-3</sup>	1.539
<i>μ</i> /mm <sup>-1</sup>	0.886
<i>θ</i> range/deg	2.85 to 26.00
Reflns collected	132254

---

Independent reflns	22720 [R(int) = 0.0810]
Params	1734
$R_1 [I > 2\sigma(I)]$	0.0603
$wR_2 [I > 2\sigma(I)]$	0.2129
Goodness of fit	0.815

---

**Table S3.** Structural Data for  $1 \cdot C_{60}$ .

	$1 \cdot C_{60}$
Tb-N(TNP) bond distance / nm	2.434
Tb-N(Pc) bond distance / nm	2.473
Tb-N <sub>4</sub> (TNP) plane distance / nm	1.246
Tb-N <sub>4</sub> Pc plane distance / nm	1.891
Interplanar distance / nm	2.801
Dihedral angle between the N <sub>4</sub> (TNP) and N <sub>4</sub> (Pc) / (°)	3.04
Dihedral angle $\phi$ for the TNP ring / (°)	12.89
Dihedral angle $\phi$ for the Pc ring / (°)	20.17
Average twist angle / (°)	44.58

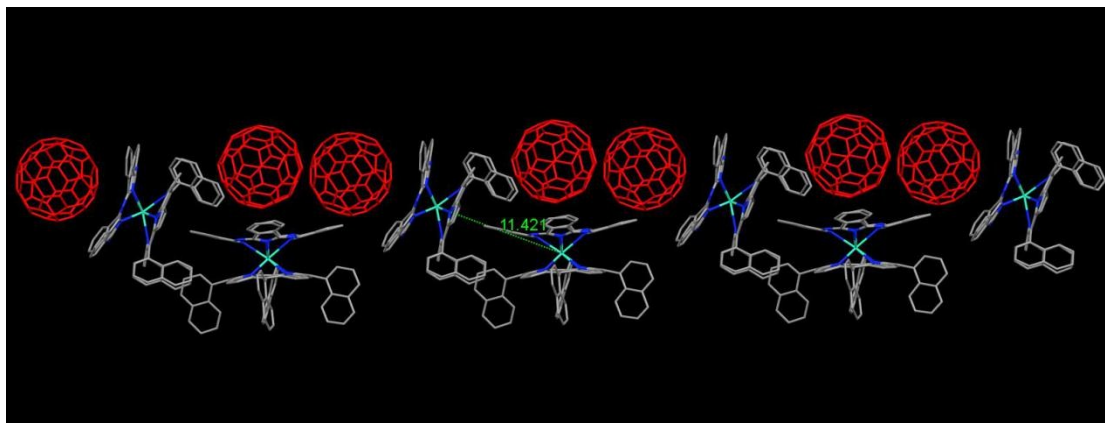


**Figure S4.** Molecular packing in single crystals of **1·C<sub>60</sub>**. Hydrogen atoms and solvent molecules are omitted for clarity.

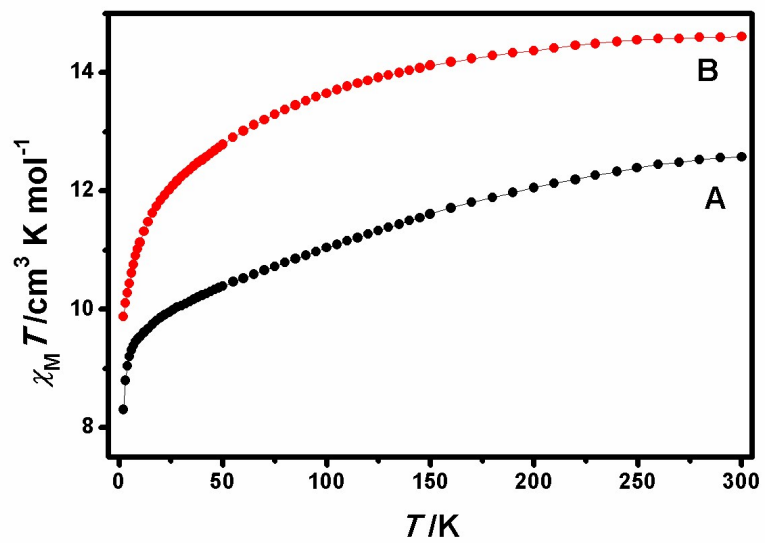


**Figure S5.** Temperature (T) dependence of  $\chi_M T$  for 1(A) and 2(B) at 1000 Oe.

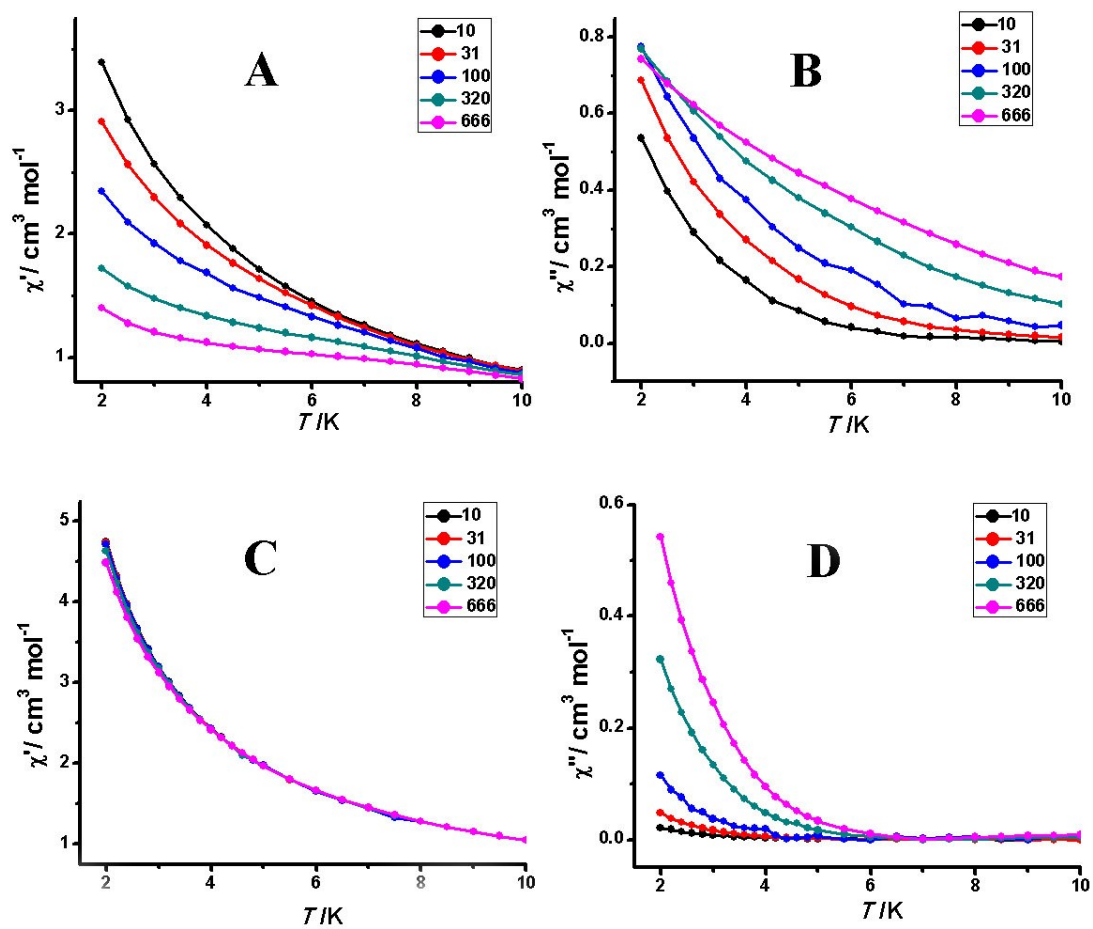


**Figure S6.** Plots for temperature dependence of the in-phase ( $\chi'$ ) and out-of-phase ( $\chi''$ ) ac susceptibility of **1** (A,B) and **2** (C, D) under a zero applied dc magnetic field.

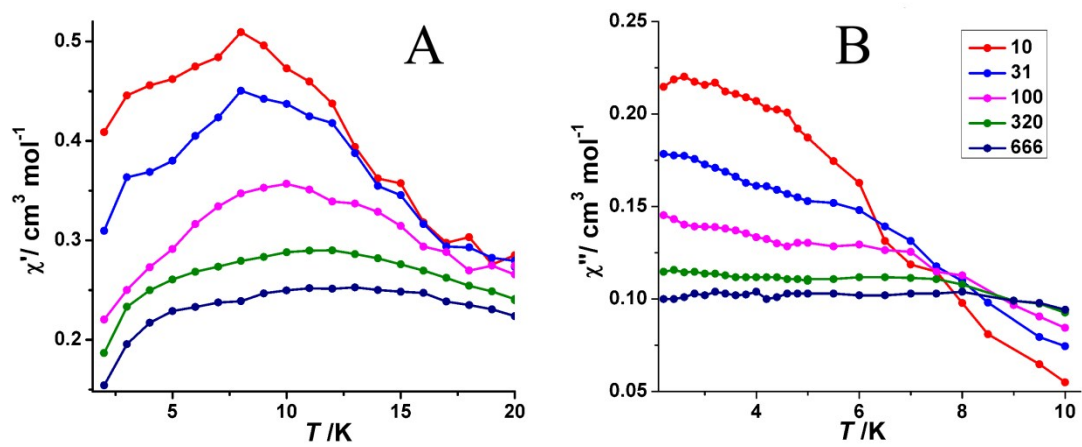


**Figure S7.** Plots for temperature dependence of the in-phase ( $\chi'$ ) (A) and out-of-phase ( $\chi''$ ) (B) ac susceptibility of **1** under 2000 Oe applied dc magnetic field.



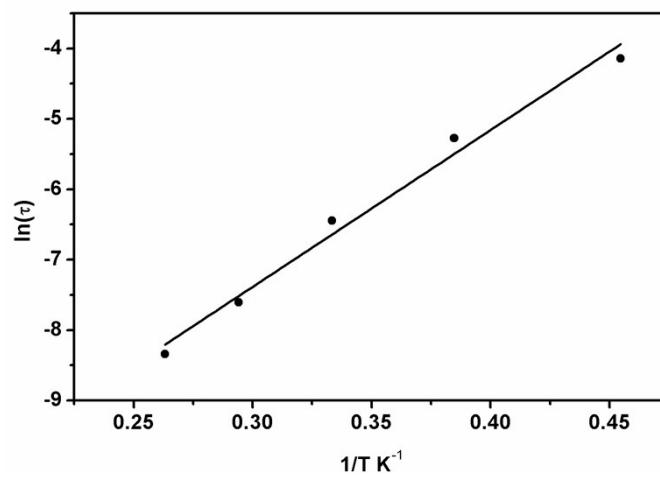


**Figure S8.** The plot of  $\ln(\tau)$  vs.  $1/T$  for **2** under 2000 Oe applied dc field.

## References

- (1). R.G. George, M. Padmanabhan, *Polyhedron*. 2003, **22**, 3145.
- (2). P.A. Barret, D.A. Frye, R.P.Linstead, *J. Chem. Soc.*, 1938, 1157.
- (3). J.G. Stites, C.N. McCarty, L.L. Quill, *J. Am. Chem. Soc.*, 1948,**70**, 3142.
- (4). SMART and SAINT for Windows NT Software Reference Manuals, Version 5.0,  
Bruker Analytical X-Ray Systems, Madison, WI, 1997.
- (5). Sheldrick, G.M. SADABS, A Software for Empirical Absorption Correction;  
University of Göttingen: Göttingen, Germany, 1997.
- (6). SHELXL Reference Manual, version 5.1; Bruker Analytical X-Ray Systems:  
Madison, WI, 1997.
- (7). S. Wang, L.Li, Z. Ouyang, Z. Xia, N. Xia, T. Peng, K. Zhang, *Acta Phys. Sin.*,  
2012, **61**, 107601.
- (8). H.Nojiri, Z. Ouyang, *Sci. Technol.*, 2012, **5**, 1.